• Basic Research •

Knockdown of fibrillin-1 suppresses retina-blood barrier dysfunction by inhibiting vascular endothelial apoptosis under diabetic conditions

Yue Zhang[1], *Xiao-Jing Liu*[2], *Xin-Ran Zhai*[2], *Yao Yao*[1], *Bin Shao*[2], *Yu-Han Zhen*[2], *Xin Zhang*[2], *Zhe Xiao*[1], *Li-Fang Wang*[1], *Ming-Lian Zhang*[1], *Zhi-Min Chen*[1]

[1]Hebei Eye Hospital, Provincial Key Laboratory of Ophthalmology, Hebei Provincial Clinical Research Center for Eye Diseases, Xingtai 054001, Hebei Province, China
[2]Department of Ophthalmology, Hebei Medical University, Shijiazhuang 050011, Hebei Province, China
Correspondence to: Ming-Lian Zhang and Zhi-Min Chen. Hebei Eye Hospital, Provincial Key Laboratory of Ophthalmology, Hebei Provincial Clinical Research Center for Eye Diseases, Xingtai 054001, Hebei Province, China. zhmlyk@sohu.com; ykyyczm@126.com
Received: 2024-01-04 Accepted: 2024-03-04

Abstract

• **AIM:** To investigate the effects of fibrillin-1 (FBN1) deletion on the integrity of retina-blood barrier function and the apoptosis of vascular endothelial cells under diabetic conditions.

• **METHODS:** Streptozotocin (STZ)-induced diabetic mice were used to simulate the diabetic conditions of diabetic retinopathy (DR) patients, and FBN1 expression was detected in retinas from STZ-diabetic mice and controls. In the Gene Expression Omnibus (GEO) database, the GSE60436 dataset was selected to analyze FBN1 expressions in fibrovascular membranes from DR patients. Using lentivirus to knock down FBN1 levels, vascular leakage and endothelial barrier integrity were detected by Evans blue vascular permeability assay, fluorescein fundus angiography (FFA) and immunofluorescence labeled with tight junction marker *in vivo*. High glucose-induced monkey retinal vascular endothelial cells (RF/6A) were used to investigate effects of FBN1 on the cells *in vitro*. The vascular endothelial barrier integrity and apoptosis were detected by trans-endothelial electrical resistance (TEER) assay and flow cytometry, respectively.

• **RESULTS:** FBN1 mRNA expression was increased in retinas of STZ-induced diabetic mice and fibrovascular membranes of DR patients (GSE60436 datasets) using RNA-seq approach. Besides, knocking down of FBN1 by lentivirus intravitreal injection significantly inhibited the vascular leakage compared to STZ-DR group by Evans blue vascular permeability assay and FFA detection. Expressions of tight junction markers in STZ-DR mouse retinas were lower than those in the control group, and knocking down of FBN1 increased the tight junction levels. *In vitro*, 30 mmol/L glucose could significantly inhibit viability of RF/6A cells, and FBN1 mRNA expression was increased under 30 mmol/L glucose stimulation. Down-regulation of FBN1 reduced high glucose (HG)-stimulated retinal microvascular endothelial cell permeability, increased TEER, and inhibited RF/6A cell apoptosis *in vitro*.

• **CONCLUSION:** The expression level of FBN1 increases in retinas and vascular endothelial cells under diabetic conditions. Down-regulation of FBN1 protects the retina of early diabetic rats from retina-blood barrier damage, reduce vascular leakage, cell apoptosis, and maintain vascular endothelial cell barrier function.

• **KEYWORDS:** diabetic retinopathy; fibrillin-1; retina-blood barrier; vascular leakage; vascular permeability; apoptosis; retinal vascular endothelial cells

DOI:10.18240/ijo.2024.08.03

Citation: Zhang Y, Liu XJ, Zhai XR, Yao Y, Shao B, Zhen YH, Zhang X, Xiao Z, Wang LF, Zhang ML, Chen ZM. Knockdown of fibrillin-1 suppresses retina-blood barrier dysfunction by inhibiting vascular endothelial apoptosis under diabetic conditions. *Int J Ophthalmol* 2024;17(8):1403-1410

INTRODUCTION

The breakdown of blood-retinal barrier (BRB) increased vascular permeability, and vascular occlusion are the main pathological changes of ocular complications of diabetes mellitus[1-2]. These complications include diabetic retinopathy (DR) and diabetes macular edema (DME). DME is a manifestation of DR, the main cause of vision loss in diabetes mellitus (DM) patients, and can occur at any stage of DR[3-4]. Within five years, there were 2%-8.2% type 2 diabetes patients

were diagnosed with DME, and this number ranges from 3.6% to 10% in China[5-6]. The pathological dysfunctions of DME lead to tissue ischemia, hypoxia, abnormal accumulation of retinal or subretinal fluid, thickening and edema of the macular area[7].

At present, the treatment for DME mainly includes laser photocoagulation therapy[8], intravitreal drug injection[9-11], and vitrectomy[12]. Due to the involvement of multiple biochemical pathways in the initiation and expansion of DME, including inflammatory factors (intercellular adhesion molecules, interleukins, *etc.*), more than 30% of patients still show poor responsiveness to simple anti-vascular endothelial growth factor (VEGF) drugs[13]. In addition, if it progresses to refractory macular edema, clinical treatment methods are even scarcer. Therefore, it is of great clinical significance to find new and effective interventional targets for treating early BRB rupture and vascular leakage in DR.

Fibrillin-1 (FBN1) is a calcium binding protein with a molecular weight of 350 kDa, forming microfibers around 12 nm in the extracellular matrix (ECM)[14]. FBN1 has the ability to interact with local transforming growth factor (TGF-β), regulate the distribution, concentration, and regulation of bone morphogenetic protein signals, as well as regulating various signaling pathways that regulate cell activity, including the formation and remodeling of ECM[15]. Although it has been reported that FBN1 has a regulatory effect on endothelial cells, there is no research evidence on the role of FBN1 in diabetes-induced macular edema, early damage of BRB function, and vascular leakage in DR. Therefore, in order to further investigate the regulatory effects of FBN1 on retinal barrier function and the integrity of retinal vascular endothelial cells, we detected the expression of FBN1 in animal models of DR and in fibrovascular membrane samples from proliferative DR (PDR) patients. By regulating the levels of FBN1 both *in vitro* and *in vivo*, we investigated its impact on vascular leakage caused by the disruption of retinal vascular barrier function. In addition, in cytological studies, the regulatory role of FBN1 on endothelial cell apoptosis was clarified.

MATERIALS AND METHODS

Ethical Approval Mice in this study were treated in accordance with approved protocols by the Laboratory Animal Management Committee at Hebei Eye Hospital (ethical approval number: 2023LW03) and followed the ARVO statement for the Use of Animals in Ophthalmic and Vision Research.

Animal Model Adult C57BL/6 male and female mice (3mo) were procured from Vital River (Beijing, China). Mice were paired, housed in standard cages within a germ-free environment, and provided with unlimited access to standard mouse chow and water. The mice were kept on a 12-h light-dark cycle, and their bedding, water, and food were refreshed every two days.

Animals were fasted for 6h before receiving intraperitoneal (*i.p.*) injections of 55 mg/kg streptozotocin (STZ) dissolved in 50 mmol/L sodium citrate buffer (pH 4.5), or an equal volume of citrate buffer alone for controls. Mice were then returned to their cages with *ad libitum* access to food and 10% sucrose/water as previously described[16]. Two weeks later, animals with fasting blood glucose ranging from 300 to 550 mg/dL were enrolled. Average body weight was monitored throughout the study.

Lentivirus (LV)-shFBN1 was conducted by BANBIO company (Shanghai, China). LV-shFBN1 was intravitreal injected 3wk after fasting blood glucose levels ranging from 300-550 mg/dL and repeated injection every week for three more weeks.

Transcription Analysis Five retinas from control and STZ-DM groups were used for RNA sequencing experiments. Total RNA was extracted using the Trizol kit (Invitrogen, Carlsbad, CA, USA) according to the manufacturer's instructions. RNA sequencing was performed by Biomarker Biotechnology Co. (Beijing, China) using a HiSeq3000 sequencing system (Illumina, San Diego, CA, USA). The quality of sequencing data was assessed using FASTQC 0.18.0. The mRNA sequences were mapped to the genome (GRCm38) using HISAT 2.2.4. Counts for each gene were extracted from the mapping file using StringTie 1.3.3. Use DESeq2 software to analyze differential RNA expression in different groups.

Data Analysis and Verification Based on GEO Database The data set GSE60436 in DR (https://www.ncbi.nlm.nih. gov/geo/) was download for searching the high-throughput Gene Expression Omnibus (GEO) database. This data set contains retinas from 3 healthy subjects, fibrovascular membranes (FVMs) from 3 PDR patients, active neovascularization (ANV) [F(A) group], and FVMs non-active neovascularization (nANV) from 3 PDR patients [F(nA) group]. After converting RNA names, the FPKM values for three groups (a total of 9 samples) corresponding to FBN1 were determined, and statistical analysis along with image generation were performed.

Evans Blue Leakage Evans blue (MedchemExpress, New Jersey, US) was diluted with phosphate buffer saline (PBS) to a concentration of 45 mg/kg and injected into the tail vein of anesthetized mice. The animals were sacrificed after 30min, the eyes were enucleated and fixed in 4% paraformaldehyde (PFA) for 30min, placed on ice for 15min, and the retinas were dissected and flattened onto a glass slide and covered. Imaging was conducted using a confocal microscope (Zeiss LSM800, Zeiss, Oberkochen, Germany), and the fluorescence intensity in each square was tracked and calculated using the Vessel J function of the NIH Image J software (version 1.8.0) with the

"fluorescence intensity ratio" input. Average values were taken and represented graphically (*n*=5 mice/group).

Fluorescein Fundus Angiography The animal was anesthetized, the pupils were dilated, and ophthalmic gel was applied to maintain corneal moisture. Each animal received an intraperitoneal injection of 220 μL fluorescein sodium (10 mL/kg, 0.5%, Alcon) solution, and fluorescein fundus vasculature imaging was performed approximately 30s after injection using a Phoenix Micron microscope (Phoenix Micro IV) with the following fluorescein fundus angiography (FFA) parameters. Contrast imaging (FFA) measurements included gain 10 dB, frame rate 15.0 fps, and exposure time 166.7ms (*n*=5 mice/group).

Cell Culture and Cell Model Development Monkey retinal vascular endothelial cells (RF/6A) were cultured with complete MEM culture medium (containing 10% fetal bovine serum and 1% penicillin/streptomyci) in a cell culture incubator at 37℃, 5% CO_2. The complete culture medium was replaced every two days.

For the development of diabetic cell model, glucose of different concentrations (0, 10, 20, 30 and 40 mmol/L) were added to the complete culture medium to simulate the high glucose condition of diabetic pathological changes. Eight hours later, cell viability, transendothelial electrical resistance (TEER), and polymerase chain reaction (PCR) were measured.

Cell Viability Measurement RF/6A cell viability was measured by cell counting kit (CCK)-8 assay. Cells were seeded in a 96-well plate. Different concentrations of glucose were added into the culture medium for 8h, 10 μL CCK-8 buffer were added into each well. After incubating for 2h, the absorbance value was measured at 450 nm.

Polymerase Chain Reaction Cells were homogenized and lysed with 1 mL TRIzol (Ambion, 15596018). Total RNA was reversed to cDNA using the superscript First-Strand Synthesis System (Thermo Fisher Scientific, K1622), according to the manufacturer's instructions. Real-time PCR was conducted using cDNA as a template, SYBER Green Master Mix (Roche, 41472600) and target genes primers. Data were analyzed using the LightCycler 480 SW1.5.1 software and $2^{-\Delta\Delta Ct}$ calculated from GAPDH as the internal control. The following gene-specific primers were used for analysis: FBN1: F-GGATACACAGGTGATGGCTTCAC, R-GTCGCATTCACAGCGGTATCCT. GAPDH: F-CCTGTTGCTGTAGCCGTATTCA, R-CCAGGT TGTCTCCTGCGACTT.

Transendothelial Electrical Resistance RF/6A cells were seeded at 5×10^5/well on culture inserts in 24-well plates (0.4 μm pore size and 6.5 mm diameter; Corning, Sigma-Aldrich, St. Louis, MO, USA). The cells were divided into 3 groups. Except for the normal group, the high glucose (HG) group and the HG+siFBN1 group were treated with HG (27 mmol/L) in the culture medium for 8h. After 8h of HG induction, culture inserts were transferred to Endohm chambers and TEER was measured using an endothelial voltage/ohmmeter (EVOM2, World Precision Instruments, Sarasota, FL, USA) as described elsewhere[16]. Net TEER was obtained after subtracting the background value and expressed as a percentage of the normal control.

RF/6A Cell Monolayer Permeability RF/6A cell monolayers were prepared in culture inserts and treated with HG and siFBN1 as described above. After 8h of treatment, transfer the inserts with cells to a new 24-well plate with 600 μL of plain RPMI 1640 in each well. The medium in the insert was replaced with 200 μL of regular RPMI containing 0.2 mg/mL fluorescein isothiocyanate (FITC)-dextran (average molecular weight 4000). After incubation for 1h at 37℃, the fluorescence intensity of the lower chamber was measured at 490 nm using an Infinite 200 PRO multimode microplate reader and the transferred FITC was obtained by subtracting the background value. Fluorescence intensity of Dextran and expressed as a percentage of ctrl group.

Flow Cytometry RF/6A was washed with cold PBS and then stained with Cycletest Plus DNA kit (Becton Dickinson, CA, USA) according to the manufacturer's instructions. Cell cycle distribution was assessed using a FACSCanto II flow cytometer (Becton Dickinson, CA, USA). Apoptosis was detected by using PE (Phycoerythrin) Annexin V Apoptosis Detection Kit (Becton Dickinson, USA). Cells were detected using an FACS flow cytometer (BD Biosciences) and analyzed using flowjo_v10 software (FlowJo LLC, USA).

Statistical Analysis All examined data were expressed as mean±standard error of mean. Statistical analysis of data was performed using IBM SPSS Statistics (SPSS Inc., Chicago, IL, USA). Comparisons between groups were performed using *t* test or one-way analysis of variance (ANOVA), followed by Fisher's least significant difference test or Dunnett T3 test. $P<0.05$ was considered significant difference.

RESULTS

Alterations in FBN1 Levels in Diabetic Retinopathy The distribution and expression of FBN1 in the eye and blood system were first reviewed. Based on the single-cell RNA expression levels of FBN1 in each tissue in the human body in human protein atlas database (https://www.proteina tlas.org)[17], the expression of FBN1 was high in horizontal cells and bipolar cells (Figure 1A). FBN1 was also distributed in various cells in the blood, including fibroblasts, macrophages, endothelial cells, smooth muscle cells, T cells, and Schwann cells. Among them, the expression level of FBN1 was highest in fibroblasts, followed by smooth muscle cells (Figure 1B).

We constructed STZ-induced DR model to simulate oxidative stress damage, vascular leakage, and other pathologies in

diabetic pathology. H&E staining showed disruption of the retinal structures, and vascular lumen in the retinal ganglion cell layer was observed in diabetic mice (Figure 2A). As shown in Figure 2B, the expression level of FBN1 in the retina of diabetic mice was significantly higher than that in the controls (P<0.01). We retrieved and analyzed the GSE60436 data set in the GEO database. Consider rephrasing: RNAseq results showed that the relative expression level of FBN1 in the retina of the healthy control group was -1.63±0.11, in the F(nA) group was -0.15±0.30, and in the F(A) group was 0.18±0.001 (Figure 2C). Compared with the control group, the expression levels of FBN1 in the F(nA) group and F(A) group were significantly increased, respectively. However, there was no statistical difference in FBN1 expression levels between the F(nA) group and the F(A) group (Figure 2D).

Retinal Vascular Leakage in Diabetic Mice Quantitative measurements after injection of Evans blue showed significant retinal vascular leakage and downregulating the expression level of FBN1 significantly reduced the leakage in the retina of STZ-DM mice (Figure 3A, 3B). The leakage levels in the STZ-DM group and STZ-DM+LV shFBN1 group were significantly higher than those in the control group (P<0.05), while the leakage levels in the STZ-DM+LV shFBN1 group were significantly lower than those in the STZ-DM group (P<0.05). FFA showed that the peripheral retinal leakage level in the STZ-DM group and STZ-DM+LV shFBN1 group was significantly increased (Figure 3C, 3D). As shown in Figure 4, zonula occludens-1 (ZO-1) expression STZ-DM group were significantly decreased compared with control group (P<0.01). ZO-1 expression in FBN1 knocking down group was significantly greater than STZ-DM group (P<0.05), but lower than control group (P<0.05). Taken together, deletion of FBN1 in STZ-DM mice ameliorated the pathological retinal vascular leakage.

HG-stimulated Retinal Microvascular Endothelial Cell Permeability and TEER after Downregulation of FBN1 The 10 and 20 mmol/L of glucose did not affect RF/6A cell viability compared to the control group (Figure 5A). However, 30 and 40 mmol/L of glucose significantly damaged cell viability compared to the control group (P<0.001, Figure 5A). Therefore, we chose 30 mmol/L of glucose to stimulate RF/6A cells in the following experiments. FBN1 mRNA expression was detected in control and 30 mmol/L glucose-treated group. As shown in Figure 5B, FBN1 was upregulated by HG stimulation compared to control group (P<0.001).

RF/6A monolayer transwell cultures showed that TEER was significantly reduced after 8h of HG treatment; while down-regulation of FBN1 in cells significantly increased TEER (Figure 6). The FITC fluorescence intensity in the HG group was significantly higher than that in the control group. Knockdown of FBN1 significantly reduced the FITC fluorescence intensity.

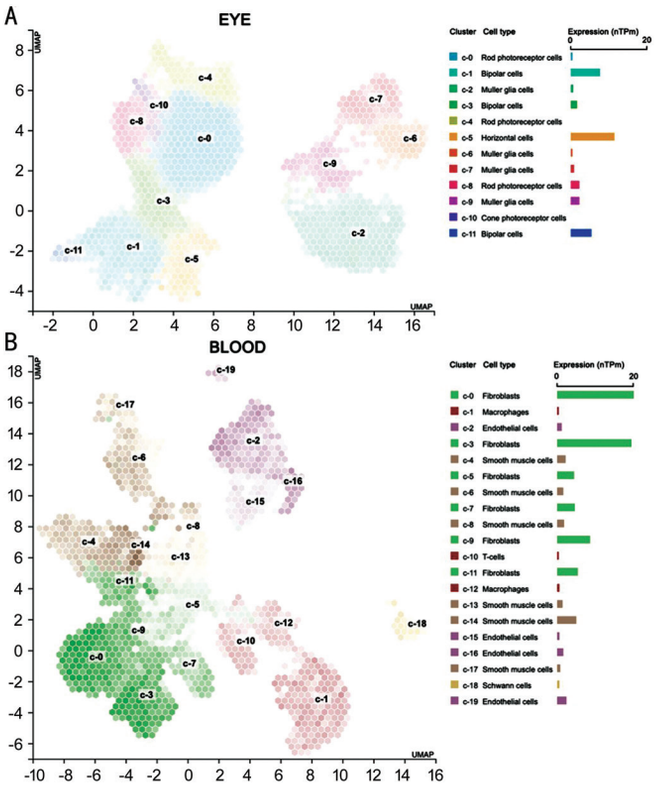

Figure 1 FBN1 distributions and expressions in ocular and blood systems Visualize RNA expression in clusters of single cell types identified in this tissue *via* UMAP plot and bar graph. UMAP-PLOT visualizes cells in each cluster, where each point corresponds to a cell. FBN1 expressions in the eye (A) and in the blood systems (B). C-0 to C-19 represent the clusters of single cell types. nTPm represents the FBN1 levels. FBN1: Fibrillin-1.

Endothelial Cell Apoptosis *in Vitro* RF/6A cells were transfected with siFBN1, induced with HG, and apoptosis was assessed by flow cytometry. HG initiated a large amount of apoptosis in RF/6A cells; while using siFBN1 to downregulate FBN1 expression in cells and alleviate the apoptosis level of endothelial cells (P<0.05; Figure 7).

DISCUSSION

The current research has clarified the expression level and cellular distribution of FBN1 in the eye and circulatory system. It has been observed that the expression level of FBN1 increases under DR and DME conditions, describing the reduction of *in vivo* and *in vitro* barrier function damage and leakage induced by high glucose by downregulating FBN1. It has been clarified that FBN1 plays its role in regulating DME by regulating endothelial cell apoptosis, thus providing potential for FBN1 as a therapeutic target for DME and DR.

FBN1 is a cysteine rich ECM glycoprotein with a size of approximately 350 kDa. Human FBN1 mutation is a major participant in various ocular components, such as the cornea, drainage tube, lens, ciliary zone, and retina[18]. According to

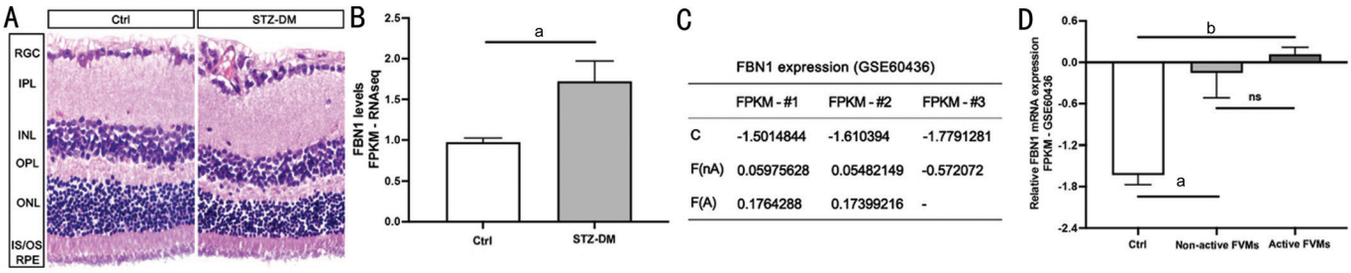

Figure 2 High expression of FBN1 in the proliferating membrane of diabetes retinopathy animal model and PDR patients A: Retinal cross section and H&E staining of control and STZ-DM animals; B: Transcriptomics method was used to detect the relative expression level of FBN1 mRNA in the retina of control group and STZ-DM group mice (*n*=5/group); C: The expression levels of FBN1 in the control group retina, PDR group FVMs ANV, and PDR group FVMs nANV in the GSE60436 dataset; D: Statistical analysis results of FBN1 expression levels in three groups of samples (*n*=3/group; ^{a}P<0.05, ^{b}P<0.0001). FBN1: Fibrillin-1; RGC: Retinal ganglion cell; IPL: Inner plexiform layer; INL: Inner nuclear layer; OPL: Outer plexiform layer; ONL: Outer nuclear layer; IS/OS: Inner and outer segment; RPE: Retinal pigmented epithelia; STZ-DM: Streptozotocin induced diabetes mellitus; PDR: Proliferative diabetic retinopathy; FVM: Fibrovascular membrane; ANV: Active neovascularization; nANV: Non-active neovascularization; Ctrl: Control.

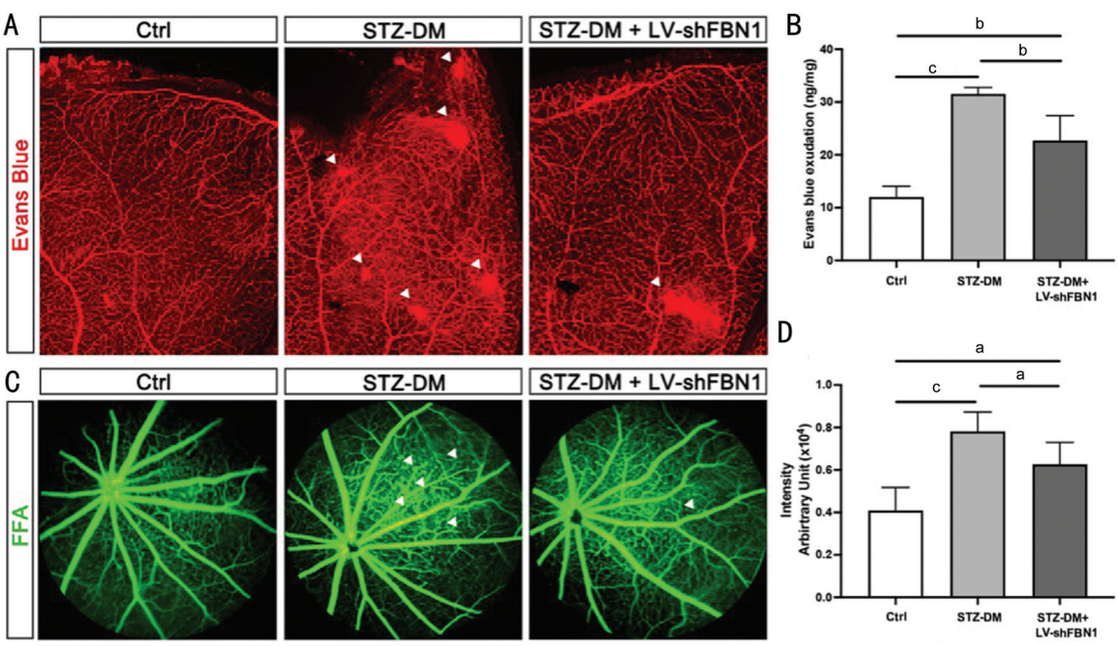

Figure 3 FBN1 affects retinal vascular permeability function *in vivo* A: Vascular permeability after Evans blue injection (*n*=5 mice/group); B: Statistical analysis of Evans blue exclusion; C: Representative images of FFA (*n*=5 mice); D: Statistical analysis of vascular fluorescence intensity (^{a}P<0.05, ^{b}P<0.01, ^{c}P<0.001). FBN1: Fibrillin-1; FFA: Fundus fluorescein angiography; STZ-DM: Streptozotocin induced diabetes mellitus; Ctrl: Control.

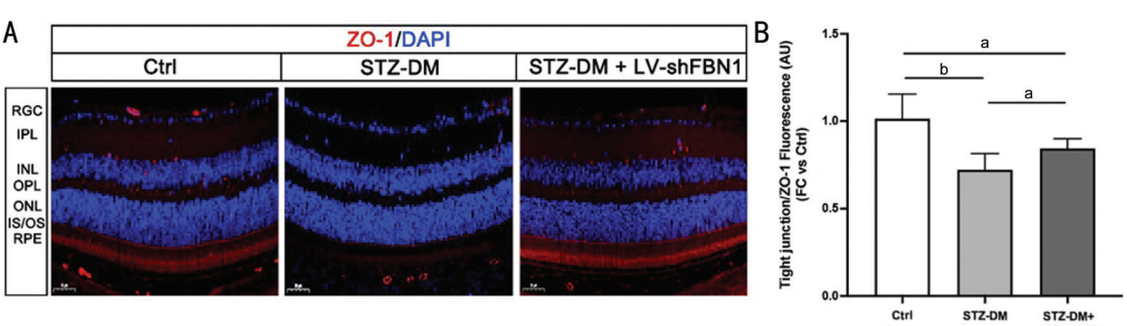

Figure 4 FBN1 affects retinal tight junction expression *in vivo* A: Representative images of retinal cross section and ZO-1 labeling demonstrating tight junctions levels affected by FBN1 (ZO-1: red; DAPI: blue); B: Statistical analysis of ZO-1 labeling (*n*=5 mice). ^{a}P<0.05, ^{b}P<0.01. FBN1: Fibrillin-1; ZO-1: Zonula occludens-1; RGC: Retinal ganglion cell; IPL: Inner plexiform layer; INL: Inner nuclear layer; OPL: Outer plexiform layer; ONL: Outer nuclear layer; IS/OS: Inner and outer segment; RPE: Retinal pigmented epithelium; STZ-DM: Streptozotocin induced diabetes mellitus; Ctrl: Control.

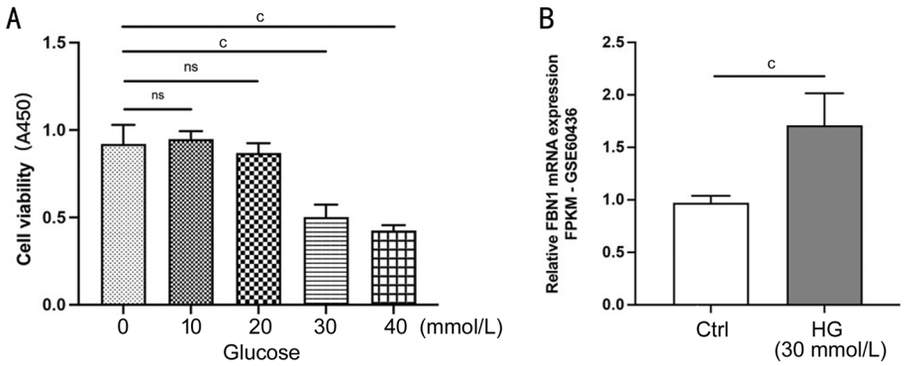

Figure 5 HG affects RF/6A cell viability and FBN1 mRNA expression A: Cell viability of RF/6A were detected of 0, 10, 20, 30 and 40 mmol/L glucose stimulation by CCK-8 assay (*n*=3/group); B: FBN1 mRNA expression in Ctrl and HG (30 mmol/L) group (*n*=3/group, [c]*P*<0.001). HG: High glucose; RF/6A: Monkey retinal vascular endothelial cells; FBN1: Fibrillin-1; CCK: Cell counting kit; Ctrl: Control.

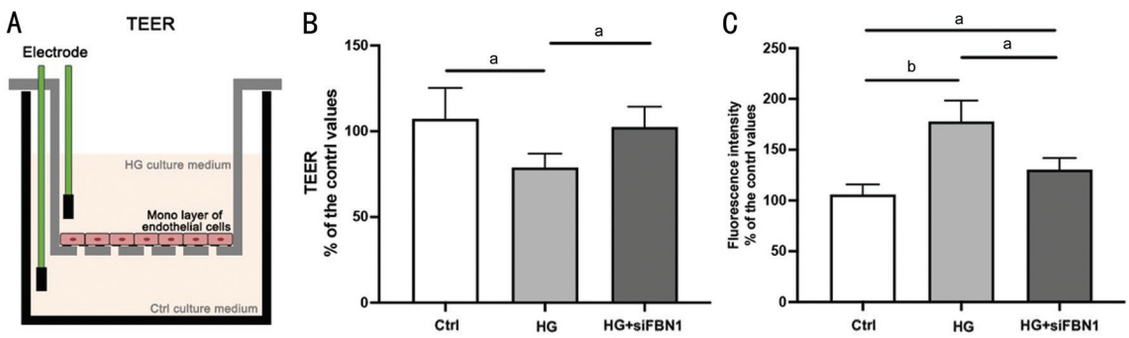

Figure 6 Knockdown of FBN1 prevents HG-induced hyperpermeability in retinal microvascular endothelial cells A: Schematic of TEER measurement; B: RF/6A cells were treated with normal or HG-containing medium, treated with siFBN1, and relative TEER was measured; C: Relative permeability was determined by the fluorescence intensity of transferred FITC-dextran on RF/6A cell monolayers ([a]*P*<0.05, [b]*P*<0.01). FBN1: Fibrillin-1; HG: High glucose; Ctrl: Control; TEER: Transendothelial electrical resistance; RF/6A: Monkey retinal vascular endothelial cells.

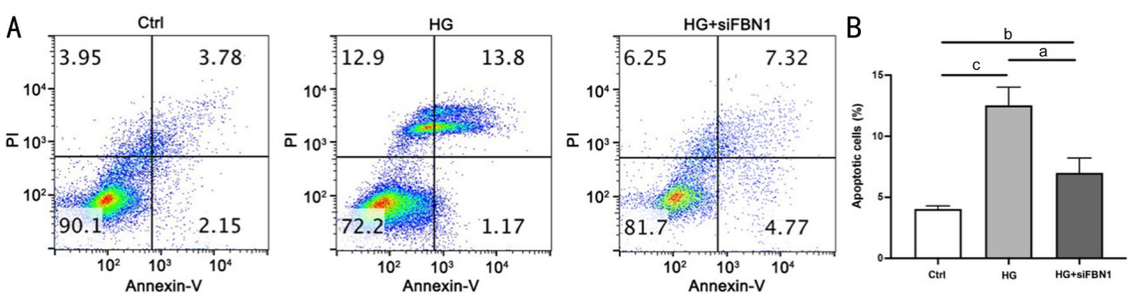

Figure 7 Downregulation of FBN1 inhibits endothelial cell apoptosis *in vitro* A: Flow cytometry shows endothelial cell apoptosis in the control group, HG-induced endothelial cell group and siRNA knockdown FBN1 group; B: Statistical analysis results of apoptotic cells ([a]*P*<0.05, [b]*P*<0.01, [c]*P*<0.001). HG: High glucose; FBN1: Fibrillin-1.

the data analysis of Human Protein Atlas, FBN1 is mainly distributed in horizontal cells and bipolar cells in the eye, as well as fibrous and smooth muscle cells in the blood circulation system. It is worth noting that FBN1 is also expressed in endothelial cells. The loss of endometrial cells and pericles and the increase of basic membrane capillaries result in paid recurrent blood flow and dysfunctional BRB. FBN1 also contains integrin receptor binding sites, which regulate gene expression, release, and activate potential TGF binding to the matrix through recombination of the cytoskeleton-β complex, inducing adaptive response to ECM changes[19].

Our results indicate that the expression level of FBN1 in the retina of DR mice is significantly increased, but there seems to be no evidence of correlation between FBN1 expression level and the occurrence of pathological neovascularization in the retina. Meanwhile, in order to clarify the relationship between FBN1 and clinical diseases and provide evidence for FBN1 as a therapeutic target for diseases such as DR and DME, we searched the GSE60436 data set in the GEO database. Samples of proliferative vascular membrane is one of the characteristics of non-proliferative DR and PDR in clinical practice. The expression level of FBN1 in proliferative vascular membrane is significantly higher than that in control group retinal tissue, indicating that FBN1 is involved in the progression of

DR disease and is correlated with the formation of clinical pathological neovascularization.

The traditional and effective Evans blue assay was used to detect and quantify the BRB decomposition and retinal vascular leakage after the onset of diabetes. This result is consistent with many reports, that is, in the STZ induced diabetes rat model, using Evans blue analysis[20-22] or other methods[22]. Therefore, BRB rupture and vascular leakage are one of the early signs of retinal damage in diabetes rats, and their pathology is similar to that of human DR[23]. The breakdown of BRB in DR and DME may be triggered by various elements, such as advanced glycation end products, VEGF, hepatocyte growth factor, TGF-β, protein kinase C, and the kallikrein-kinin system, which exhibit heightened levels in the hyperglycemic environment[24]. Our study demonstrated vascular leakage and BRB breakdown in diabetic mice retinas. Knocking down FBN1 expression *in vivo* can reverse retinal leakage and barrier function damage in STZ-DM mice. The endothelium of the BRB establishes intricate junction complexes that govern cellular permeability. Tight junctions intertwine with adhesive junctions on endothelial cells, and they develop subsequent to the formation of adhesive junctions[25]. ZO-1 stands out as one of the most notable connecting proteins thus far, acting as a bridging protein that links with the cytoskeleton[26]. It may contribute to cell contraction, thereby exerting control over the dynamic opening of tight junctions. We found that ZO-1 expressions decreased in STZ-DM group, as expected, and ZO-1 levels increased after FBN1 deletion, suggesting that FBN1 regulates tight junction expression and BRB function in DR mice.

In addition, downregulation of FBN1 can restore cell barrier function and reduce cell leakage in monolayer retinal vascular endothelial cells cultured *in vitro*. Endothelial cells provide a non-thrombotic monolayer surface arranged in the lumen of blood vessels, serving as the cell interface between blood and tissue[27]. TEER is a widely accepted quantitative technique used to measure the integrity of tight junction dynamics in endothelial and epithelial monolayer cell culture models. Before evaluating the transportation of drugs or chemicals, the TEER value is a powerful indicator of cell barrier integrity. Some barrier models widely characterized by TEER include BRB, gastrointestinal tract, and lung models[28-30]. Furthermore, knockdown of FBN1 declines endothelial cell apoptosis and rebuild endothelial cell survival, leading to rescue the disruption of retinal vascular integrity and microvascular sparsity.

However, there are several shortcomings in this study. First, we found that FBN1 mRNA levels in F(nA) and F(A) group were significantly higher compared that in control group based on GSE60436 datasets, but there is no direct FBN1 staining and location information in control human eyes and fibrovascular membrane from DR patients. Second, a positive control for FBN1 knocking is important to indicate the effects of FBN1 on RF/6A cells.

In conclusion, the expression level of FBN1 increases under DR and DME pathological conditions. Downregulation of FBN1 can protect the retina of early diabetes rats from BRB damage, reduce vascular leakage, reduce endothelial cell apoptosis, and maintain endothelial cell barrier function.

ACKNOWLEDGEMENTS

Authors' contributions: Zhang Y and Chen ZM designed the study; Zhang Y, Liu XJ and Zhai XR performed the experiments and wrote the manuscript; Yao Y, Shao B, and Zhen YH analyzed the data; Zhang X, Xiao Z, and Wang LF performed H&E and IF staining; Zhang ML and Chen ZM Chen provided the funding for the research.

Foundations: Supported by the Xingtai Key Research and Development Projects (No.2022zz073); the Hebei Key Research and Development Projects (No.23377712D).

Conflicts of Interest: Zhang Y, None; **Liu XJ,** None; **Zhai XR,** None; **Yao Y,** None; **Shao B,** None; **Zhen YH,** None; **Zhang X,** None; **Xiao Z,** None; **Wang LF,** None; **Zhang ML,** None; **Chen ZM,** None.

REFERENCES

1 Maurissen TL, Spielmann AJ, Schellenberg G, Bickle M, Vieira JR, Lai SY, Pavlou G, Fauser S, Westenskow PD, Kamm RD, Ragelle H. Modeling early pathophysiological phenotypes of diabetic retinopathy in a human inner blood-retinal barrier-on-a-chip. *Nat Commun* 2024;15(1):1372.

2 Gong QY, Hu GY, Yu SQ, Qian TW, Xu X. Comprehensive assessment of growth factors, inflammatory mediators, and cytokines in vitreous from patients with proliferative diabetic retinopathy. *Int J Ophthalmol* 2022;15(11):1736-1742.

3 Gonzalez-Cortes JH, Martinez-Pacheco VA, Gonzalez-Cantu JE, Bilgic A, de Ribot FM, Sudhalkar A, Mohamed-Hamsho J, Kodjikian L, Mathis T. Current treatments and innovations in diabetic retinopathy and diabetic macular edema. *Pharmaceutics* 2022;15(1):122.

4 Zhang JF, Zhang JX, Zhang CY, Zhang JT, Gu LM, Luo DW, Qiu QH. Diabetic macular edema: current understanding, molecular mechanisms and therapeutic implications. *Cells* 2022;11(21):3362.

5 Ding J, Wong TY. Current epidemiology of diabetic retinopathy and diabetic macular edema. *Curr Diabetes Rep* 2012;12(4):346-354.

6 Virgili G, Menchini F, Casazza G, Hogg R, Das RR, Wang X, Michelessi M. Optical coherence tomography (OCT) for detection of macular oedema in patients with diabetic retinopathy. *Cochrane Database Syst Rev* 2015;1(1):CD008081.

7 Munk MR, Somfai GM, de Smet MD, Donati G, Menke MN, Garweg JG, Ceklic L. The role of intravitreal corticosteroids in the treatment of DME: predictive OCT biomarkers. *Int J Mol Sci* 2022;23(14):7585.

8 Everett LA, Paulus YM. Laser therapy in the treatment of

diabetic retinopathy and diabetic macular edema. *Curr Diab Rep* 2021;21(9):35.

9 Shimizu N, Oshitari T, Tatsumi T, Takatsuna Y, Arai M, Sato E, Baba T, Yamamoto S. Comparisons of efficacy of intravitreal aflibercept and ranibizumab in eyes with diabetic macular edema. *Biomed Res Int* 2017;2017:1747108.

10 Choi KS, Chung JK, Lim SH. Laser photocoagulation combined with intravitreal triamcinolone acetonide injection in proliferative diabetic retinopathy with macular edema. *Korean J Ophthalmol* 2007;21(1):11-17.

11 Heng LZ, Sivaprasad S, Crosby-Nwaobi R, Saihan Z, Karampelas M, Bunce C, Peto T, Hykin PG. A prospective randomised controlled clinical trial comparing a combination of repeated intravitreal Ozurdex and macular laser therapy versus macular laser only in centre-involving diabetic macular oedema (OZLASE study). *Br J Ophthalmol* 2016;100(6):802-807.

12 Ivastinovic D, Haas A, Weger M, Seidel G, Mayer-Xanthaki C, Lindner E, Guttmann A, Wedrich A. Vitrectomy for diabetic macular edema and the relevance of external limiting membrane. *BMC Ophthalmol* 2021;21(1):334.

13 Nguyen QD, Brown DM, Marcus DM, Boyer DS, Patel S, Feiner L, Gibson A, Sy J, Rundle AC, Hopkins JJ, Rubio RG, Ehrlich JS, RISE and RIDE Research Group. Ranibizumab for diabetic macular edema: results from 2 phase III randomized trials: RISE and RIDE. *Ophthalmology* 2012;119(4):789-801.

14 Zhang RM, Zeyer KA, Odenthal N, Zhang YY, Reinhardt DP. The fibrillin-1 RGD motif posttranscriptionally regulates ERK1/2 signaling and fibroblast proliferation via miR-1208. *FASEB J* 2021;35(5):e21598.

15 Halper J. Basic components of connective tissues and extracellular matrix: fibronectin, fibrinogen, laminin, elastin, fibrillins, fibulins, matrilins, tenascins and thrombospondins. *Adv Exp Med Biol* 2021;1348:105-126.

16 Wan L, Li J, Chen WB, Wu GQ. Beneficial effects of protocatechuic acid on diabetic retinopathy in streptozocin-induced diabetic rats. *Int J Ophthalmol* 2023;16(6):855-862.

17 Ni YW, Teng T, Li RT, Simonyi A, Sun GY, Lee JC. TNFα alters occludin and cerebral endothelial permeability: role of p38MAPK. *PLoS One* 2017;12(2):e0170346.

18 Hubmacher D, Reinhardt DP, Plesec T, Schenke-Layland K, Apte SS. Human eye development is characterized by coordinated expression of fibrillin isoforms. *Invest Ophthalmol Vis Sci* 2014;55(12):7934-7944.

19 Olivieri J, Smaldone S, Ramirez F. Fibrillin assemblies: extracellular determinants of tissue formation and fibrosis. *Fibrogenesis Tissue Repair* 2010;3(1):24.

20 Fang MY, Wan WC, Li QM, Wan WW, Long Y, Liu HZ, Yang X. Asiatic acid attenuates diabetic retinopathy through TLR4/MyD88/NF-κB p65 mediated modulation of microglia polarization. *Life Sci* 2021;277:119567.

21 Zhang JF, Wu YL, Jin Y, Ji F, Sinclair SH, Luo Y, Xu GX, Lu L, Dai W, Yanoff M, Li WY, Xu GT. Intravitreal injection of erythropoietin protects both retinal vascular and neuronal cells in early diabetes. *Invest Ophthalmol Vis Sci* 2008;49(2):732-742.

22 Shi FJ, Xie H, Zhang CY, Qin HF, Zeng XW, Lou H, Zhang L, Xu GT, Zhang JF, Xu GX. Is Iba-1 protein expression a sensitive marker for microglia activation in experimental diabetic retinopathy? *Int J Ophthalmol* 2021;14(2):200-208.

23 Kim SR, Im JE, Jeong JH, Kim JY, Kim JT, Woo SJ, Sung JH, Park SG, Suh W. The cKit inhibitor, masitinib, prevents diabetes-induced retinal vascular leakage. *Invest Ophthalmol Vis Sci* 2016;57(3):1201.

24 Klaassen I, Van Noorden CJF, Schlingemann RO. Molecular basis of the inner blood-retinal barrier and its breakdown in diabetic macular edema and other pathological conditions. *Prog Retin Eye Res* 2013;34:19-48.

25 Yu S, Cui K, Wu P, Wu B, Lu X, Huang R, Tang X, Lin J, Yang B, Zhao J, He Q, Liang X, Xu Y. Melatonin prevents experimental central serous chorioretinopathy in rats. *J Pineal Res* 2022;73(1):e12802.

26 Robles-Osorio ML, Sabath E. Tight junction disruption and the pathogenesis of the chronic complications of diabetes mellitus: a narrative review. *World J Diabetes* 2023;14(7):1013-1026.

27 Radwan B, Prabhakaran A, Rocchetti S, Matuszyk E, Keyes TE, Baranska M. Uptake and anti-inflammatory effects of liposomal astaxanthin on endothelial cells tracked by Raman and fluorescence imaging. *Mikrochim Acta* 2023;190(8):332.

28 Srinivasan B, Kolli AR, Esch MB, Abaci HE, Shuler ML, Hickman JJ. TEER measurement techniques for *in vitro* barrier model systems. *J Lab Autom* 2015;20(2):107-126.

29 Peskar D, Kerec Kos M, Cerkvenik U, Nemec Svete A, Erman A. Sex-dependent differences in blood-urine barrier are subtle but significant in healthy and chronically inflamed mouse bladders. *Int J Mol Sci* 2023;24(22):16296.

30 Wongwanakul R, Aueviriyavit S, Furihata T, Gonil P, Sajomsang W, Maniratanachote R, Jianmongkol S. Quaternization of high molecular weight chitosan for increasing intestinal drug absorption using Caco-2 cells as an *in vitro* intestinal model. *Sci Rep* 2023;13(1):7904.